THE JOURNAL OF BIOLOGICAL CHEMISTRY
Vol. 272, No. 29, Issue of July 18, pp. 18350–18357, 1997

Printed in U.S.A.

Phosphorylation Controls the Three-dimensional Structure of Plant Light Harvesting Complex II*

(Received for publication, February 25, 1997, and in revised form, April 30, 1997)

Anders Nilsson‡, Dalibor Stys‡§, Torbjörn Drakenberg¶, Michael D. Spangfort§‖, Sture Forsén¶, and John F. Allen‡‡‡**

From ‡Plant Cell Biology, Box 7007, Lund University, S-220 07 Lund, ¶Physical Chemistry 2, Box 124, Lund University, S-221 00 Lund, and ‖Biochemistry, Box 124, Lund University, S-221 00 Lund, Sweden

The most abundant chlorophyll-binding complex in plants is the intrinsic membrane protein light-harvesting complex II (LHC II). LHC II acts as a light-harvesting antenna and has an important role in the distribution of absorbed energy between the two photosystems of photosynthesis. We used spectroscopic techniques to study a synthetic peptide with identical sequence to the LHC IIb N terminus found in pea, with and without the phosphorylated Thr at the 5th amino acid residue, and to study both forms of the native full-length protein. Our results show that the N terminus of LHC II changes structure upon phosphorylation and that the structural change resembles that of rabbit glycogen phosphorylase, one of the few phosphoproteins where both phosphorylated and non-phosphorylated structures have been solved. Our results indicate that phosphorylation of membrane proteins may regulate their function through structural protein-protein interactions in surface-exposed domains.

Light harvesting complex II (LHC II)[1] is a major chlorophyll-containing protein complex that accounts alone for half of the pigments involved in photosynthesis in plants. It is located mainly in appressed regions of the thylakoid membrane where it acts as the light-harvesting antenna for photosystem II (PS II). Reversible phosphorylation of LHC II is an established mechanism for redistribution of absorbed light energy between PS II and PS I. Phosphorylation of LHC II (giving LHC II(P)) is triggered by conditions where the plastoquinone pool of the photosynthetic electron transport chain becomes reduced (1). The kinase responsible for the phosphorylation of LHC II is not yet identified, although it is suggested that it is located in the core of photosystem II (2) or in contact with the cytochrome b_6f complex (3, 4). LHC II(P) is found in the unappressed regions of the chloroplast thylakoid membrane and there acts as a light-harvesting antenna for photosystem I (PS I) (5–7). From electron crystallography of 2-dimensional crystals, a structure for the major part of non-phosphorylated LHC II has been described at 3.4-Å resolution (8). This structure reveals no information regarding the N-terminal domain that contains the phosphorylation site at position 5 (Thr); the protein backbone was traced only to residue 26 where it ends up close to the lipid membrane, consistent with the fact that the sequence between residues 21 and 29 (RVKYLGPF) (9) consists mainly of hydrophobic, aromatic, or charged amino acids. Aromatic residues are located at the membrane surface in structures of membrane proteins (10–13), and residues Trp-16 and Tyr-17 of LHC II may also then form a point of contact with the membrane. LHC II has been shown to lose its ability to trimerize when more than the first 15 amino acids are removed from the apoprotein (14). At this site, specific lipid-protein interactions between the amino side chains and the lipid *phosphatidylglycerol* are involved in stabilization of the trimers (15), which implies that only the first 15 amino acid residues at the N terminus may be free of competing interactions with the membrane. This sequence (RKSAT*TKKVASSGSP, where * denotes the phosphorylation site, Thr-5) contains numerous positive charges, which may be compensated by the negative charge introduced by phosphorylation. To see whether a structural change occurs within the N-terminal domain itself, we have studied a synthetic peptide with the N-terminal sequence normally found in pea (9) with and without Thr-5 synthetically phosphorylated. We have also studied native LHC II/LHC II(P) from pea to see if there exists a structural analogy between the peptides and the native protein. Our results show that phosphorylation causes a structural change both in the model peptide and at the N terminus of LHC II itself, together with dissociation of the trimer aggregate. Specific changes in structure-dependent protein-protein as well as lipid-protein interactions must therefore be the basis of the mechanism by which phosphorylation controls the functional interactions of LHC II *in vivo*.

EXPERIMENTAL PROCEDURES

Peptide Synthesis and Protein Purification—The synthetic peptides RKSATTKKVASSGSP (1585.5 Da) and the corresponding phosphorylated form RKSAT(PO_3)TKKVASSGSP (1664.5 Da) were synthesized as described earlier (16). For the Fourier transform infrared (FTIR) and circular dichroism (CD) measurements, full-length proteins of LHC II were isolated from pea leaves (*Pisum sativum* L.) according to standard protocols (17, 18). Normally 100 g of pea leaves were harvested, and each batch of thylakoids was then divided into two; one, giving phospho-LHC II, was then illuminated (130 μmol m^{-2} s^{-1} for 20 min) in the presence of 0.4 mM ATP (Sigma) and 25 mM NaF (Sigma). The same purification protocol was followed for both samples, except that all buffers contained 10 mM NaF in the purification yielding phospho-LHC II. This preparation contained a mixture of both phosphorylated and non-phosphorylated LHC II; the proportion of LHC II(P) was determined by mass spectroscopy to be approximately 10%. For simplicity the phosphorylated preparation will from herein be denoted as LHC II(P).

* This work was supported by the Swedish Natural Sciences Research Council (NFR), Eric and Ulla Schyberg Foundation, the EC DG XII SCIENCE program, and Federation of European Biochemical Societies. The costs of publication of this article were defrayed in part by the payment of page charges. This article must therefore be hereby marked "*advertisement*" in accordance with 18 U.S.C. Section 1734 solely to indicate this fact.

§ Present address: Institute of Microbiology, Academy of Science of the Czech Republic, CZ-379 01 Trebon, Czech Republic.

** ALK Labs, Bøge Allé 10–12 DK-2970 Hørsholm, Denmark.

‡‡ To whom correspondence should be addressed. Tel.: 46-46 2227788; Fax: 46-46 2223684; E-mail: john.allen@plantcell.lu.se.

[1] The abbreviations used are: LHC II, light harvesting complex II; PS II, photosystem II; PS I, photosystem I; LHC II(P), phosphorylated light harvesting complex II; FTIR, Fourier transform infrared; ATR, attenuated total reflection; NOE, nuclear Overhauser effect; standard 1- and 3-letter abbreviations for the amino acid residues.

UV Absorption Measurements—Static solvent perturbation UV absorption measurements of LHC II(P) and LHC II were performed on a double-beam Hitachi U-3000 (Hitachi Ltd, Japan); equal concentrations dissolved in 20 mM Tris buffer (pH 8.0) or H_2O were used as sample and reference, respectively. Ethanol was then added to give up to 10% (v/v) in both sample and reference, and difference spectra were measured between 200 and 300 nm at a resolution of 0.1 nm. All difference spectra showed zero absorbance in the region 200–600 nm, before ethanol addition. The difference spectrum is the average of five individual, but nearly identical, difference spectra, each from one sample preparation (five non-phosphorylated and five phosphorylated), and the resulting spectra were then co-added and averaged. Standard spectra of L-tyrosine and L-tryptophan (Sigma) solutions in Tris buffer or H_2O with additional ethanol were used to confirm the origin of the increase in absorbance at 280 nm upon solvent perturbation. Identical solutions in the sample and reference cuvettes were used to check the samples for inhomogeneity; no spectral difference between samples was then seen either before or after addition of ethanol.

CD Measurements—The circular dichroism (CD) spectra were obtained on a JASCO 720 (Japan Spectroscopic Co. Ltd, Tokyo, Japan) spectrophotometer at 25 °C, using an 8.0 mM, 0.1 mM, or 0.8 μM protein solution in a quartz cuvette with an optical path length of 1 mm. The scan velocity was 1 nm s^{-1} in the frequency range between 180 and 250 nm, and each spectrum consists of eight scans. The spectra shown are the average of four, each from an individual sample, and with the water background subtracted. The relative contribution of each secondary structural motif was calculated with software supplied with the spectrophotometer (19). Solutions of LHC II and LHC II(P) were measured between 350 and 750 nm to determine the oligomeric state (20) but were otherwise under the same conditions as those described above.

FTIR Measurements—FTIR spectra were recorded at a Bruker IFS 66 (Karlsruhe, Germany) spectrometer using a liquid N_2 cooled MCT detector. 2000 scans were collected and Fourier transformed to obtain a spectral resolution of 2 cm^{-1} in the spectral region 4000–600 cm^{-1}. The spectra were measured using a horizontal attenuated-total-reflection (ATR)-crystal (45°) (ZnSe). Peptide solution (approximately 75 μl, 0.8 μM (pH 5.2)) was spread out on the internal reflection crystal and then the sample holder was sealed to avoid evaporation of water. All peptides were washed repeatedly with either H_2O or D_2O (Sigma), followed by rotary evaporation using a Speedvac (Savant Industries, Farmingdale, NY) to dry the peptide between washes, to remove traces of the trifluoroacetic acid used during peptide purification. The H_2O/D_2O exchange of LHC II was performed on a dried sample by addition of 70 μl of D_2O to the protein film. The exchange was followed by sequential measurements of 100 scans (30 s) during a period of 2 h. The film was then repeatedly dried and rehydrated with D_2O to obtain full H_2O/D_2O exchange. All the difference spectra are the average of eight individual spectra, each from one sample preparation (four non-phosphorylated and four phosphorylated), and each individual spectrum is the signal average of 2000 scans. Spectral deconvolution (LabCalc-Galactic Industries Corp., Salem, NH) and derivation were performed. The number of bands and the peak positions thereby obtained were used to calculate (PeakFit-Jandel Scientific Software, San Rafael, CA) a curve fit that is composed of Lorenzian bands for the original IR absorbance band. In the case of H_2O, an interactive spectral subtraction was performed to remove the spectral influence of the δ-mode of bulk water, positioned at 1645 cm^{-1}. All FTIR measurements were performed at 22 °C.

NMR Measurements—All nuclear magnetic resonance (NMR) spectra were acquired at 500 MHz on a GE Omega 500 spectrometer (General Electric, Fremont, CA). Spectra were obtained of aqueous peptide solutions (8 mM). pH was established by addition of small volumes of HCl or NaOH solution in the case of measurements in H_2O or of deuterium chloride or sodium deuteroxide in D_2O for measurements in deuterated solution; the peptide solutions were self-buffering. All NMR spectra were recorded at 2 °C. To obtain a temperature dependence of the NH chemical shift for the phosphorylated peptide at pH 5.2, TOCSY spectra were recorded at 5, 17, and 25 °C. TOCSY spectra were acquired using the MLEV sequence (21) with a mixing time of 120 ms, at 2048 data points with 16 repetitions and 256 τ_1 values. ROESY spectra (22) were acquired with a mixing time of 200 ms, at 2048 or 4096 data points with 32 repetitions and 256 τ_1 values. Nuclear Overhauser enhancement spectroscopy spectra (23) were acquired with a mixing time of 500 ms, at 2048 data points with 32 repetitions and 256 τ_1 values. Sequential assignment was carried out by methods of Wüthrich (24). One-dimensional spectra were recorded for both peptides at concentrations 8.0, 2.0, 0.5, and 0.1 mM, and no changes were observed in line shape or line position.

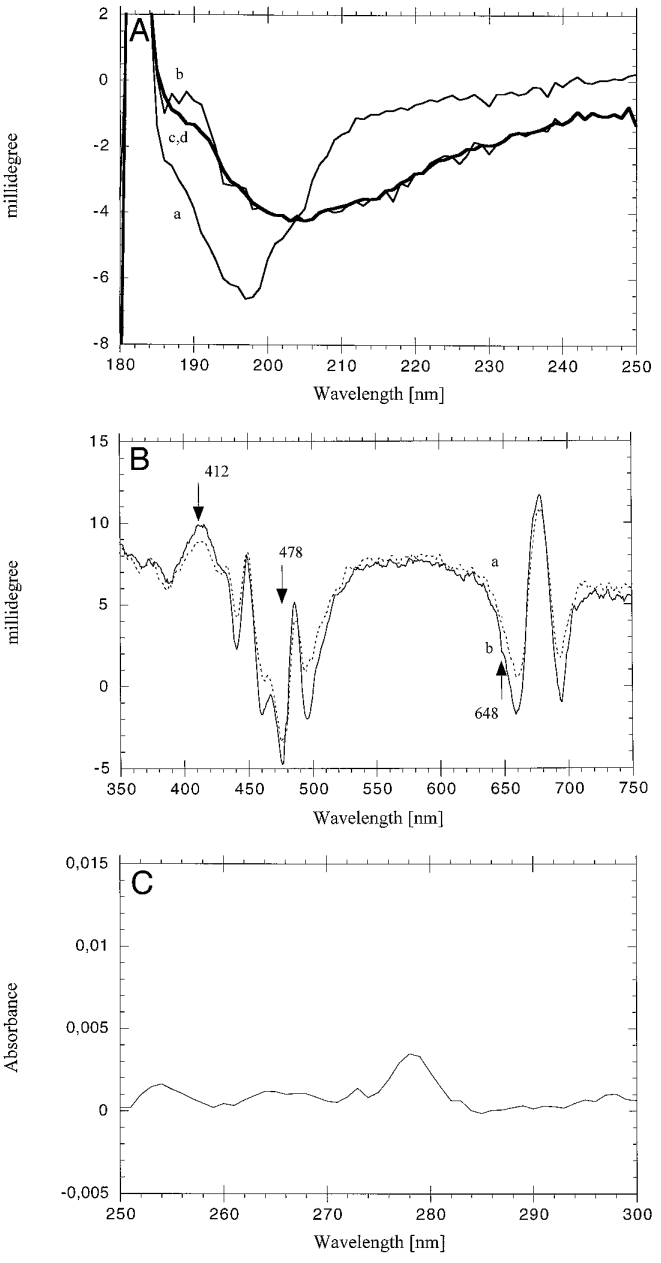

FIG. 1. **UV-visible spectra.** *Panel A* shows CD spectra of the phosphorylated (*a*) and the non-phosphorylated peptide (*b*) at 0.8 μM and at 8 mM (*c* and *d*) in the wavelength region 180–250 nm. *Panel B* shows CD spectra of LHC II(P) (*trace a, dotted line*) and LHC II (*trace b, solid line*) in the wavelength region 350–750 nm. The shoulder characteristic of the trimeric form of LHC II is found at 648 nm (20). *Panel C* shows the solvent pertubation difference spectrum of LHC II(P)/LHC II in the region 250–300 nm. The proteins are resuspended in 20 mM Tris buffer (pH 8.0), and ethanol is added to give a final concentration of 10% (v/v). Further details are given under "Experimental Procedures."

RESULTS

CD, NMR, and FTIR Spectroscopy of LHC II Peptides—All three spectroscopic methods revealed distinct differences between the non-phosphorylated and phosphorylated forms of a 15-residue peptide corresponding to the N-terminal phosphorylation site of LHC II. CD spectra clearly show differences in conformation between the two peptides in monomeric solution (0.8 μM) (Fig. 1*A*). The phosphorylated peptide contains α-helix, a structural type that is absent from the non-phosphorylated form (see Table I). The α-helix content of 12%, which corresponds to only 2 amino residues, in the phosphorylated peptide

TABLE I

Showing the calculated relative amount or relative area representing the different classes of secondary protein structures

The results are from the nonphosphorylated 15-mer peptide and the phosphorylated 15-mer peptide, presented above in that order.

Peak assignment	CD-calculated relative amount	FTIR relative peak area	FTIR peak position
	%	%	cm^{-1}
Aggregated strand	56/15	52/54	1620–1630
α-Helix	0/12	2/23	≈1655
β-Sheet	20/25	38/19	1670–1680
β-Turn	21/19	7/3	1698

is not sufficient to form a complete α-helical turn. The β-structure content is constant at around 45% for the two peptides, but the random coil content is decreased in the phosphorylated peptide by the same amount (12%) as the increase in α-helix. CD measurements made at the same concentration range (8.0–0.1 mM) as the NMR spectra (see below) show almost identical spectra (Fig. 1*A*) for the two peptides, both being rather similar to the spectrum of the non-phosphorylated peptide at lower concentrations. These spectra indicate mainly random coil structures with some β-structure contribution. The difference between the two sets of concentrations indicates that the peptides aggregate at higher concentrations, and intermolecular interaction is thereby introduced.

Most of the NMR spectra were taken of an 8 mM self-buffering solution, under conditions in which the CD spectra of both the phosphorylated and non-phosphorylated peptides were identical. Upon stepwise dilution down to 0.1 mM, neither the position of the resonances nor the line shape changed, which indicates that the structure remains unchanged and the eventual aggregates remain intact.

The NMR spectra of the non-phosphorylated peptide are largely independent of pH, whereas the spectra of the phosphorylated peptide change significantly in the pH range 4.0–7.5 (Fig. 2). We analyzed the spectra corresponding to residues 2–14 taken at pH values 4–5.6 and residues 3–14 at pH 6.2. At higher pH, the exchange rate of the backbone NH protons was too fast to enable analysis of the spectrum other than to assign the spin systems on the basis of their analogy with the resonances in the spectrum taken at lower pH.

In all NMR spectra, the number of spin systems exceeds the expected number deduced from the primary structure. In the non-phosphorylated peptide (Fig. 3*A*), doubling occurred of the spin system of Gly-13, whose NH protons appear at 8.45 and 7.9 ppm. In the corresponding ROESY spectrum, a strong sequential cross-peak for Gly-13(8.45)-αH-Ser-14-NH is present, whereas only a Gly-13(7.9)-NH Ser-14-NH cross-peak can be observed, and not the corresponding αH-NH cross-peak. The Lys-7(8)βH-Ser-14-NH cross-peak can also be identified for the non-phosphorylated peptide.

For the phosphorylated peptide we confine our discussion to the spectra measured at pH 6.2, the highest pH at which a spectrum could reasonably be interpreted (Fig. 3*B*) and the pH closest to the physiological value (pH 8). In addition, the spectra at pH values in the range 4.2–5.6 are complicated by the existence of a number of minor spin systems that probably arise from minor structures in slow exchange. Many spectral features of the non-phosphorylated peptide are seen also for the phosphorylated peptide. A new position appeared for the Gly-13 spin system resonances which is indicated by the cross-peak with coordinates 8.12 and 3.45. We could observe only a weak Gly(8.12)-NH-Ser-14-NH sequential cross-peak in the non-phosphorylated peptide. Distinct differences were found, not surprisingly, for the residues Thr-5 and Thr-6.

The NMR spectra of the phosphorylated peptide contained

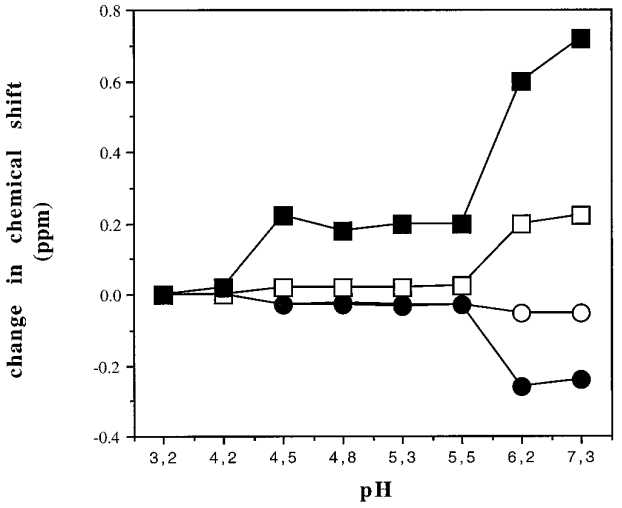

FIG. 2. **pH dependence of the chemical shifts.** The chemical shift of the residues Thr-5 and Thr-6 in the phosphorylated peptide as a function of pH is shown. The proton chemical shifts of the more populated structures are shown. ○, αH Thr-6; ●, αH Thr-5; □, NH Thr-6; ■, NH Thr-5.

many unique cross-peaks. These are difficult to assign unambiguously, since the peptide obviously adopted more than one conformation (Fig. 4).

Fig. 5 shows the FTIR spectral region of the C=O stretch vibration of the peptide backbone, normally denoted as the amide I band (1580–1750 cm^{-1}) or amide I′ when studies are performed in deuterated solvent. The dihedral angles of the peptide backbone determine the geometry of the backbone. Different backbone geometries thus imply different lengths and strengths of the hydrogen bonds involving C=O groups. The different characteristic amide I frequencies arise from the variation in length and direction of these hydrogen bonds correlated with the different structures. Different peak positions have been assigned through both empirical and theoretical work to different structural motifs of the peptide backbone (25). Bands located around 1650–1658 cm^{-1} correspond to α-structures (26) or, as found in some cases, loops (27), whereas bands centered around 1620–1640 and 1680–1689 cm^{-1} are due to β-structures (28, 29), and those at around 1690–1700 cm^{-1} are due to β-turns (30). Fig. 5 shows the FTIR spectra of the non-phosphorylated (*panel A*) and phosphorylated (*panel B*) peptide (*trace a* in H_2O, *trace b* in D_2O), together with the 2nd derivative spectrum (*trace c*), the Fourier self-deconvoluted spectrum (*trace d*), and the individual spectral components (*traces e*) from the curve fitting procedure, respectively. As can be seen, deuterated and H_2O-subtracted spectra are in a very good agreement. Furthermore, both the Fourier self-deconvoluted and the 2nd derivative spectra indicate identical numbers of bands and band positions. Table I lists the relative band areas and peak positions obtained for the different spectral components and their correspondence to different structural classes. The relative area of an infrared absorption band can, as a first approximation, be assumed to be a measure of the relative amount of that particular component. However, this assumption does not take into account absorption by amino acid side chains, or the slightly different extinction coefficients of different structural motifs (31–33). The most conspicuous difference between the FTIR spectra of the phosphorylated and the non-phosphorylated peptides is that the phosphorylated peptide contains a definite contribution from α- structure that is absent from that of the non-phosphorylated form (Table I). Furthermore, the large contribution of β-turn structure in the non-phosphorylated peptide is much lower in the phosphoryl-

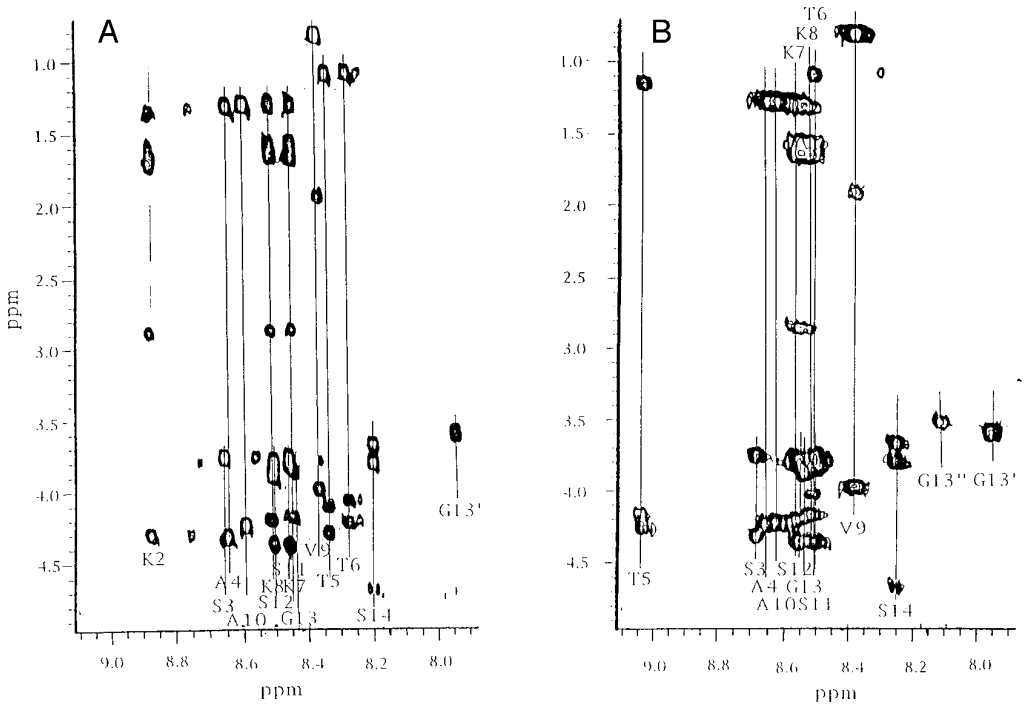

FIG. 3. **Detail of the 500-MHz TOCSY spectra.** Spectra of the peptide RKSATTKKVASSGSP (*A*) and the peptide RKSAT(PO_3)TKKVASSGSP (*B*) at pH 5.3. Only those spin systems that may be clearly assigned to the main or minor conformation are indicated. *Prime* indicates the spin systems belonging to the less populated conformation. *T5** is probably the spin system of the double charged phosphorylated threonine residue. This assignment is based solely on the comparison to spectra at higher pH.

ated form.

Structural Effect of Phosphorylation of LHC II by FTIR, CD, and UV Solvent Perturbation Spectroscopy—In addition to information obtained from synthetic peptides corresponding to the LHC IIb N terminus, we have performed studies of the native protein. Fig. 6 shows the amide I band region of the ATR-FTIR spectra of LHC II and LHC II(P), together with the difference spectrum. These absorbance bands are the sum of absorbances from each amino acid in the protein, and the first 15 amino acid residues of the N terminus contribute only as a part of the full structure of 234 amino acids. The main absorbance band is located at 1653 cm^{-1}, indicating mainly an α-helical structure, which is in agreement with the model based on electron diffraction (8). A second band is also shown in the figure at around 1550 cm^{-1} and is assigned to the delocalized amide II vibration. This band has a more complex origin and is therefore not interpreted here. Even though the individual spectra seem to be identical, the difference spectrum shows significant changes. The positive peaks in the difference spectrum reflect structures more abundant in the non-phosphorylated protein than in the phosphorylated protein, and vice versa. For the samples measured in H_2O, the positive band located at around 1625 cm^{-1} is assigned to β-strand structures, whereas the negative bands at 1678 cm^{-1} and 1652 cm^{-1} are assigned to β-turns and α-helices, respectively. H_2O/D_2O exchange experiments (Fig. 6*B*) confirm that the 1652-cm^{-1} band originates from an α-like structure and not from a random or unordered structure (25), since deuteration has no effect on this band even after 2 h, indicating no direct contact with the surrounding solvent. Furthermore, the deuteration effect on the amide II band (delocalized C—N—H bending mode) at 1550 cm^{-1} confirms the assumption that part of LHC II is exposed to the surrounding medium and is not embedded in the membrane. After exposure to D_2O for only 5 min, approximately 25% of the total area of that band is shifted to 1465 cm^{-1}, corresponding to 25% of the protein accessible for rapid H/D exchange. The hydrophobic segments inside the membrane and coiled structures outside the membrane are prevented from such exchange, and only a minor increase of exchanged protons can be found even after 2 h exposure. Interestingly, the negative 1652 cm^{-1} band in the D_2O difference spectrum is the only one of the three major bands found in H_2O difference spectrum that remains at the same positions in both solvents. The absolute area of the difference bands in this region is approximately 4% of the total area in the absorbance spectrum.

The FTIR results demonstrate that LHC II(P) has a higher content of α- and β-turn structures and a lower content of β-stranded structures than the non-phosphorylated form of LHC II. The protein segments that cause the 1625- and 1678-cm^{-1} bands are located outside the membrane domain of non-phosphorylated LHC II. The protein segment that causes the 1652-cm^{-1} band originates from an α-structure present only in LHC II(P). The total number of amino acid residues participating in these changes is in the order of 5–10 amino residues.

CD in the wavelength region 350–750 nm has been suggested as an assay for the oligomeric state of native protein (20): the trimeric form of LHC II has a characteristic negative shoulder in the CD spectrum at 648 nm, and further but less significant differences were found at 412 and 478 nm between the monomeric and trimeric forms of LHC II. LHC II(P) CD spectra measured here have a less pronounced shoulder at 648 nm than the LHC II spectra (Fig. 1*B*) together with spectral features typical for the monomeric form of LHC II at the other two wavelengths. Studies of the minor light-harvesting chlorophyll-*a*/*b*-binding protein CP 29 (Lhc b4) have shown that increased chlorophyll *b* content will enhance a negative signal at 648 nm in the CD spectrum (34). Our findings thus indicate that dissociation of the trimer and phosphorylation may perturb the chlorophyll b_2 or b_3 (8) in the same way. This suggests that phosphorylation induces dissociation of LHC II trimers. The samples here denoted LHC II(P) contain around 90% of non-phosphorylated LHC II (see "Experimental Procedures") and would therefore be expected to show only 10% of the decrease of the 648 nm signal of LHC II, as observed (Fig. 1*B*).

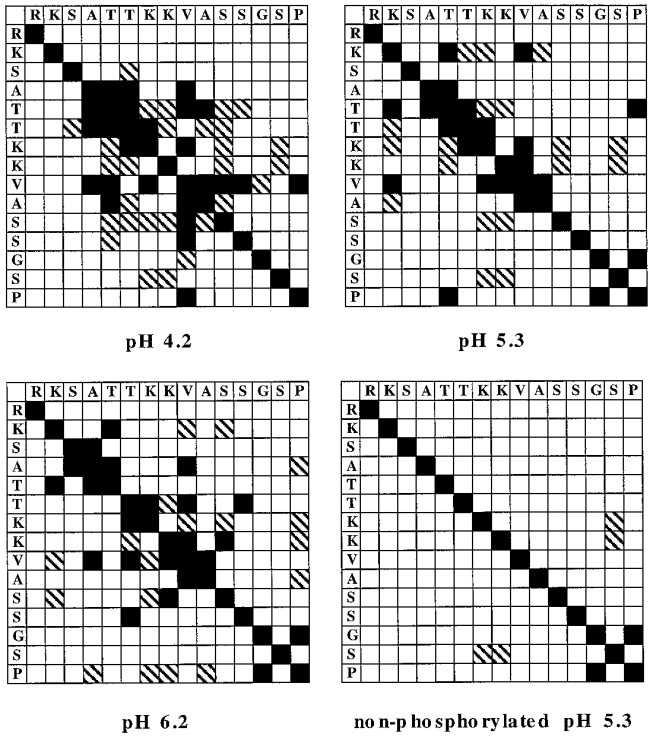

FIG. 4. **Summary of the structural information obtained by NMR spectroscopy.** The NOE constraints observed in the spectra of the peptide at pH 4.2, 5.3, and 6.2 for the phosphorylated form and at pH 5.3 for the non-phosphorylated peptide. A *filled square* in the figure indicates that one or more NOE constraints was observed between protons of the residue defined by the coordinates in the scheme. A *hatched square* indicates ambiguous assignment. In all cases only side chain-to-backbone constraints are observed, with the exception of Lys-7(8) γH to Val-9γH NOE at pH 6.2. Only those constraints that are assigned to the more populated structure are taken into account.

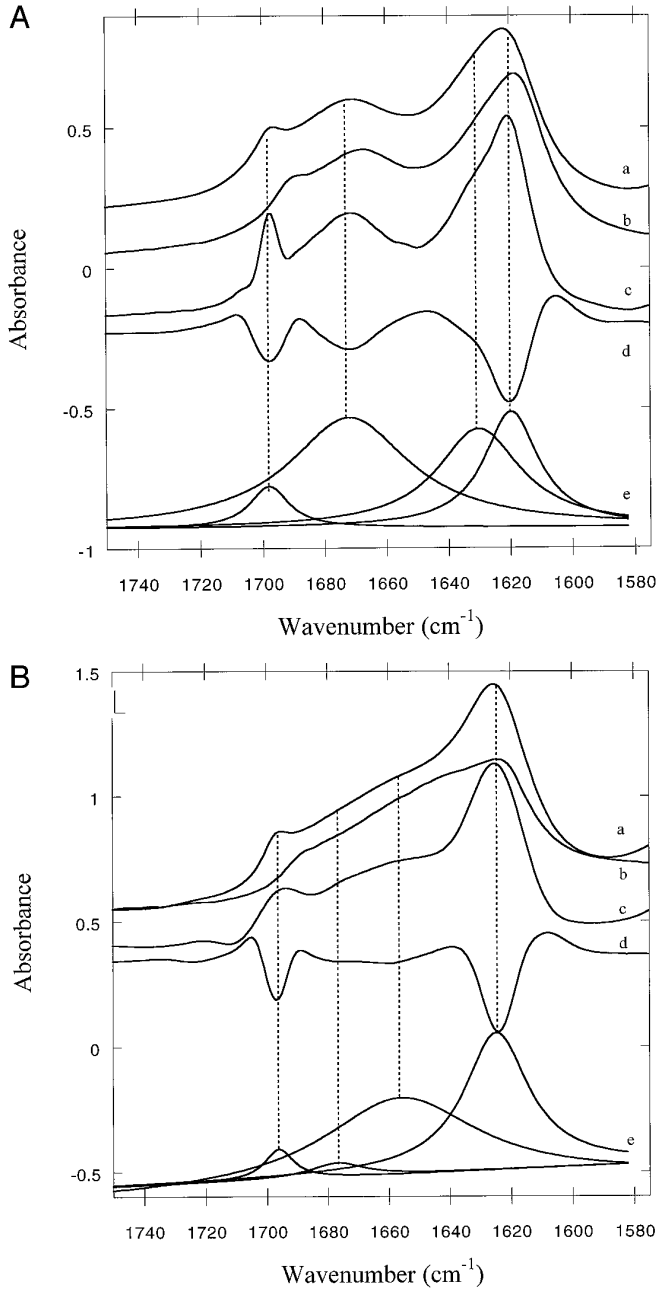

FIG. 5. **The FTIR spectra of the peptide in the amide I region.** ATR-FTIR spectra of the non-phosphorylated peptide (*panel A*), and the phosphorylated peptide (*panel B*). In both panels, *trace a* is the spectrum measured in H_2O after interactive subtraction of bulk water, and *trace b* is the spectrum obtained when the peptide is dissolved in D_2O and no subtraction is performed. *Trace c* is the Fourier self-deconvoluted H_2O spectrum (66), using a *k* value of 2.4 and (*d*) is the 2nd derivative of the H_2O spectrum. The *e traces* are the results of a curve fit performed on the original IR band measured in H_2O, using the number of bands and peak positions obtained from *traces c* and *d* as initial starting values.

Aromatic amino acid residues (Trp, Phe, and Tyr) absorb light in the UV region. Their absorption spectra may be perturbed by change in the polarity of the environment, *e.g.* by adding glycerol or ethanol. Membrane-embedded, or otherwise buried, residues will, however, not be affected to the same degree by changes in the solvent. Such solvent perturbation was used here to study the differences in number of buried aromatic residues between the LHC II and LHC II(P). After an addition of 10% (v/v) ethanol, to samples of LHC II and LHC II(P) at equal concentrations, a positive peak is found in the difference spectrum LHC II(P)/LHC II at around 280 nm (Fig. 1*C*). Both Tyr and Trp groups have stronger absorbance at 280 nm when dissolved in ethanol than when dissolved in H_2O. This implies that the phosphorylated samples of LHC II have more aromatic amino acid residues exposed to the surrounding medium than the non-phosphorylated samples.

DISCUSSION

Other studies of subunits of phosphoproteins or phosphopeptides (35–43) have shown local structural alteration upon phosphorylation in some cases but not in others. Of these examples, the chlorophyll protein 29 subunit of PS II is most closely related to LHC II. There is independent evidence for a conformational change upon phosphorylation of chlorophyll protein 29 (43). Previous structural studies of LHC II (8, 44) have produced no direct structural information about the phosphorylation site. Indirectly, it has been found that proteolytic removal of the first 8 amino acid (44) residues does not affect the trimerization of LHC II but removal of the first 49 does. It has therefore been proposed (44) that the segment of 8 amino acids at the N terminus is disordered and has no structural role of the formation of trimers. However, the study was carried out only on LHC II and not on LHC II(P). LHC II(P) has not so far been found in the trimeric state, which is the only state that has been crystallized. The formation of two-dimensional and three-dimensional crystals has been shown (44) to depend on specific lipid-protein interactions. Specifically, the region around residue 16 (Pro-**Trp**-Tyr-Gly-Pro) has been shown to interact with the lipids phosphatidylglycerol (14, 15), monogalactosyl diacylglycerol, and digalactosyl diacylglycerol. Crystal formation is also dependent on the relative concentra-

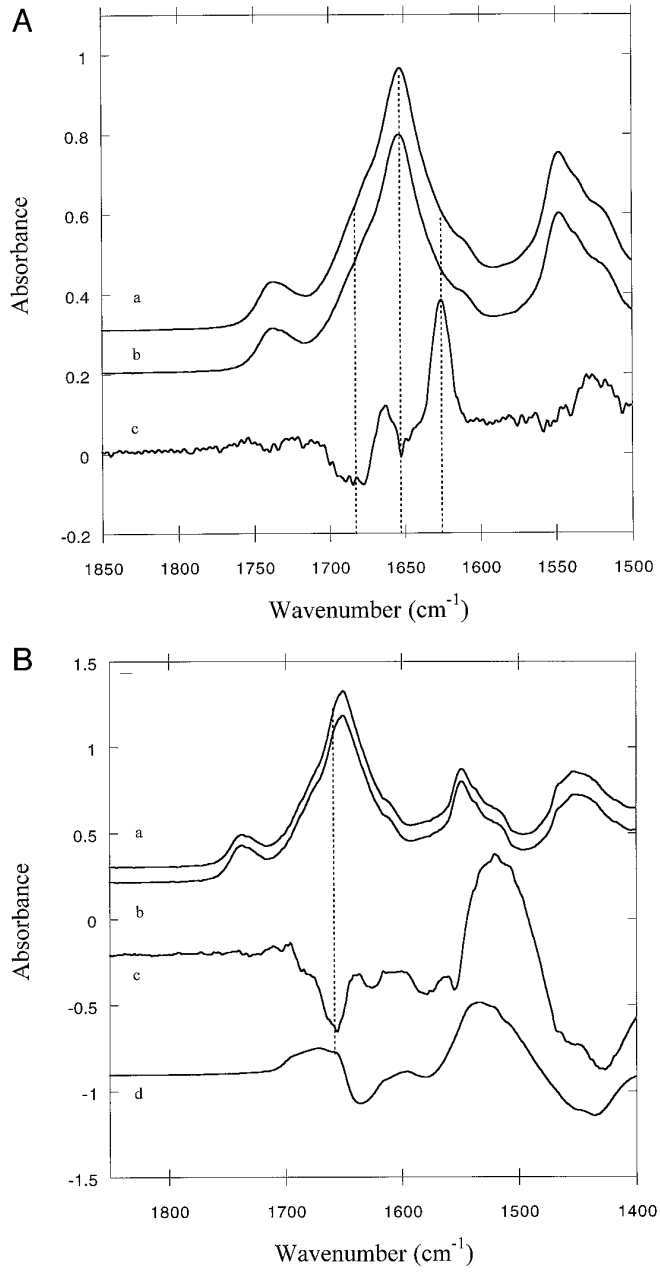

FIG. 6. **The FTIR spectra of LHC II/LHC II(P) in the amide I region.** ATR-FTIR spectra of LHC II (*trace a*)/LHC II(P) (*trace b*) in H_2O (*panel A*) and in D_2O (*panel B*). The difference spectra (*trace c*) were obtained by subtracting the LHC II(P) spectrum from that of LHC II and is scaled 50 times compared with the absolute absorbance spectra (*a* and *b*). In *panel B*, *trace d* is the H/D difference spectrum of LHC II, showing the effect of the H/D exchange on the amide I and II bands.

tion of the last two lipids. Monogalactosyl diacylglycerol is a non-lamellar phase-triggering lipid (for review of this area, see Ref. 45), whereas digalactosyl diacylglycerol forms bilayers or reversed hexagonal phases depending on the acyl chain composition. Furthermore, modification of the C-terminal end of LHC II (46) has been shown to be important for stabilization of the protein, particularly of the pigment-protein complex.

Our results clearly show that peptides corresponding to the N terminus of LHC II and LHC II(P) have non-random tertiary structure although the backbones are mostly extended. Furthermore, we found that the peptides can form stable dimers, and the NMR data indicate that the phosphate group of Thr-5 forms a hydrogen bond to the NH proton of Thr-6. In glycogen phosphorylase (47), a similar hydrogen bond between the phosphate group on Ser-14 and backbone NH of Val-15 is observed. Surprisingly, other protons in the N-terminal region of the peptide were affected only marginally. We also have an indication from the other spectroscopic techniques that the phosphate group interacts with surrounding amino acid residues and thereby alters the structure. The phosphate group also decreases the tendency of the peptides to aggregate. The discrepancy between the amount of the secondary structural motif, particularly the lower values of β-structure and higher content of random coil obtained from the CD compared with the FTIR measurements (see Table I), is similar to that described for other proteins (27, 28, 48) and may be attributed to the different sensitivities of the different methods and problems with structural classification of very small peptide segments. The CD spectrum actually reflects the asymmetric conformation of the single L-amino acid peptide backbone, whereas the FTIR spectrum reflects the environmental effects on the C=O bond of the peptide backbone. We conclude that the full-length LHC II exhibits structural differences between its phosphorylated and non-phosphorylated forms that are similar to those of the model peptide; upon phosphorylation of LHC II, an extended structure is replaced by a short, helix-like structure and by a β-turn. These changes are confined to parts of the protein extrinsic to the membrane.

The band at 1652 cm^{-1}, which is characteristic of a helix, may be assigned to the local structure around Thr-5, in agreement with our findings that the phosphorylated peptide has such a structure around its phosphorylation site. Such a structural change is similar to that seen in the crystal structures of rabbit glycogen phosphorylase in its non-phosphorylated and phosphorylated forms (47). The structural information obtained from the peptides in this investigation may not reflect a totally accurate protein backbone conformation. In the case of glycogen phosphorylase (47) the change in local structure induces a global structural change involving subunit interaction and cofactor binding. Our findings of enhanced β-turn content in LHC II(P) may thus indicate a similar global structural change upon phosphorylation of LHC II. Furthermore, our solvent perturbation measurements show that LHC II has a higher number of aromatic amino acid residues associated with the hydrophobic membrane domain than LHC II(P). Residue 16 is Trp and residue 17 is Tyr. It is therefore plausible to assume that these aromatic amino acid residues are the ones that are shielded by the lipids in the non-phosphorylated LHC II, whereas upon phosphorylation of the N terminus, they are exposed to the surrounding medium. Thus, a good candidate for the β-turn site is the same region as that at which the phosphatidylglycerol interaction has been shown to take place. There are two prolines located at positions 15 and 19. Prolines are able to *cis-trans*-isomerize, and a total isomerization of these two prolines would induce a complete turn of the protein backbone. Proline groups are also known to induce hinges in different proteins (49–51). Such relocation of the negatively charged phosphate group can move it closer to the highly positively charged region around the helix-membrane interface (see Fig. 7). This model would then also explain why LHC II(P) is not found as trimers and hence does not crystallize. The interaction between phosphatidylglycerol and the region around residue 16 was shown to be of importance for trimerization and thereby crystal formation. In LHC II(P) this lipid-protein interaction is broken by structural and interactional changes.

The Functions of LHC II and LHC II(P)—As discussed above, our results imply a quaternary and tertiary structural change upon phosphorylation of LHC II. We propose a model, shown in Fig. 7, describing the events of phosphorylation and protein

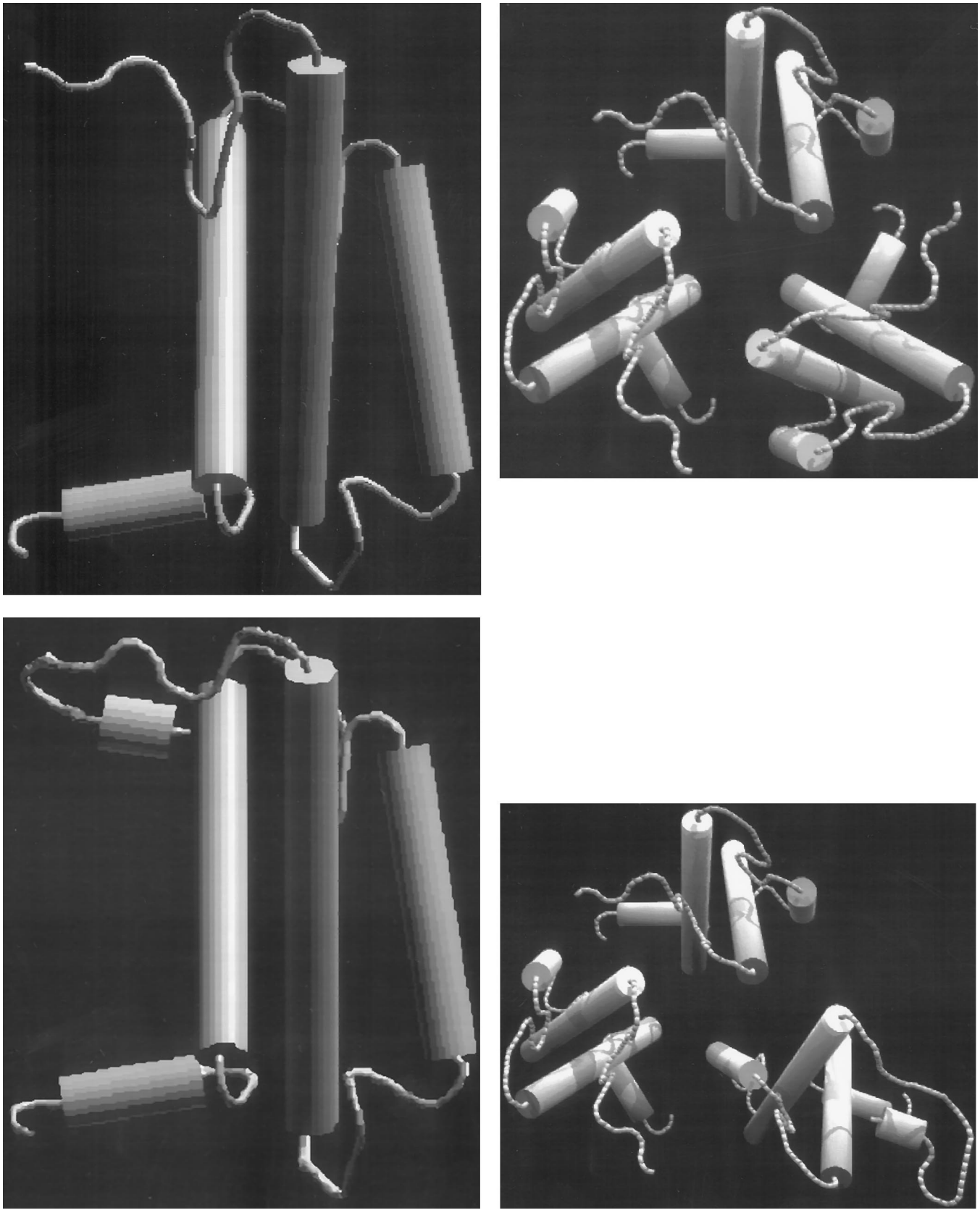

FIG. 7. **Schematic structural models of LHC II/LHC II(P).** The figure shows a simplified model of the effect of phosphorylation at the Thr-5 of LHC II. The structural model is based on coordinates of the helix-α-carbon in LHC II, kindly given to us by W. Kühlbrandt (8). The positions of the loops and the proposed new structure around the phosphorylation site are arbitrary. The *left panel* shows the protein viewed perpendicular to the normal of the membrane in two different rotations around the *y* axis, with the non-phosphorylated protein in the *upper half* and the phosphorylated protein in the *lower half*. The *right panel* shows a top view of the proposed effect of dissociation of the trimers by the phosphorylation of LHC II whereby LHC II/LHC II(P) becomes free to diffuse. Since unstacking of thylakoids will enhance the diffusion rate of proteins (57), the probability of finding the phosphorylated form of the protein, with its lower affinity for the trimer and PS II, is higher in nonstacked than in stacked thylakoids. See "Discussion" for further details.

migration. The tight complex between LHC II and PS II is based on specific protein-protein/protein-lipid interactions, which include the phosphorylation site. The regulatory effects of phosphorylation of LHC II are decoupling of adjacent thylakoids, destacking of the membranes, and migration and docking of LHC II(P) with PS I (5). Dephosphorylation of LHC II(P) has the opposite effects. These effects have previously been proposed to depend mainly on simple electrostatic repulsion and/or attraction (52), where the addition of the negatively charged PO_4 group induces a repulsive force between opposing, stacked thylakoids and, to reduce that force, LHC II(P) migrates laterally into unappressed regions of membrane. However, earlier it has been shown that photosystem segregation and membrane stacking are separate events (53). Furthermore, it has been shown that importing LHC II into stacked and unstacked thylakoid membranes causes the LHC II in the unstacked regions to migrate toward the PS II-rich stacked regions and not in the opposite direction toward regions with high density of PS I complexes (54). This result is in agreement with LHC II and LHC II(P) having different affinities for the two photosystems. The findings of dimer formation by the non-phosphorylated peptide and dissociation of the dimer by phosphorylation may help to explain the role of phosphorylation in destacking of the thylakoid membranes.

Our results are more in favor of an explanation of control of LHC II function based on structural changes (5, 55, 56), reducing the distance of electrostatic effects to short range, intramolecular interactions. The tertiary structure of LHC II may have a higher affinity for PS II than that of LHC II(P) and a lower affinity for PS I, and migration of LHC II between PS II and PS I will then be simply a result of normal lateral diffusion (57). Structures have now been obtained for some of the primary components of photosynthetic light harvesting (8, 58–60), reaction centers (10, 61–63), and secondary electron transfer and CO_2 assimilation (64, 65). Further work can now logically be directed at an atomic resolution description of the structural changes involved in regulation of light harvesting in photosynthesis, where the complexes involved are intrinsic to photosynthetic membranes.

Conclusions—The results presented here imply that regulation of light-harvesting by means of phosphorylation of chloroplast LHC II can be understood in terms of effects of the phosphate group on protein structure and on molecular recognition. This conclusion removes a conceptual barrier between regulation of ligand binding in soluble proteins and regulation of the function of membrane proteins, where, in photosynthesis at least, emphasis has been placed on the effect of protein phosphorylation on net membrane surface charge. Our results indicate that understanding regulation of photosynthesis will likewise depend on a full three-dimensional structural description of effects of post-translational, covalent modification.

Acknowledgments—We thank Drs. H. Franzén and I. Blaha for the synthetic peptides used, Dr. L. Cheng for the help with preparation of LHC II and LHC II(P), and Dr. P.-O Arvidsson for drawing Fig. 7.

REFERENCES

1. Ghanotakis, D. F., Demetriou, D. M., and Yocum, C. F. (1987) *Biochim. Biophys. Acta* **891,** 15–21
2. Race, H. L., and Hind, G. (1996) *Biochemistry* **35,** 13006–13010
3. Gal, A., Herrmann, R. G., Lottspeich, F., and Ohad, I. (1992) *FEBS Lett.* **298,** 33–35
4. Vener, A. V., van Kan, P. J. M., Gal, A., Andersson, B., and Ohad, I. (1995) *J. Biol. Chem.* **270,** 25225–25232
5. Allen, J. F. (1992) *Biochim. Biophys. Acta* **1098,** 275–335
6. Allen, J. F., Bennett, J., Steinback, K. E., and Arntzen, C. J. (1981) *Nature* **291,** 25–29
7. Larsson, U. K., Jergil, B., and Andersson, B. (1983) *Eur. J. Biochem.* **136,** 25–29
8. Kühlbrandt, W., Wang, D. N., and Fujiyoshi, Y. (1994) *Nature* **367,** 614–621
9. Cashmore, A. R. (1984) *Proc. Natl. Acad. Sci. U. S. A.* **81,** 2960–2964
10. Deisenhofer, J., Epp, O., Miki, K., Huber, R., and Michel, H. (1985) *Nature* **318,** 618–624
11. Weiss, M. S., and Schulz, G. E. (1992) *J. Mol. Biol.* **227,** 493–509
12. Henderson, R., Baldwin, J. M., Ceska, T. A., Zemlin, F., Beckman, E., and Downing, K. H. (1990) *J. Mol. Biol.* **213,** 899–929
13. Tsukihara, T., Aoyama, H., Yamashita, E., Tomizaki, T., Yamaguchi, H., Shinzawa-Itoh, K., Nakashima, R., Yaono, R., and Yoshikawa, S. (1996) *Science* **269,** 1069–1074
14. Hobe, S., Förster, R., Klinger, J., and Paulsen, H. (1995) *Biochemistry* **34,** 10224–10228
15. Trémolières, A., Dainese, P., and Bassi, R. (1994) *Eur. J. Biochem.* **221,** 721–730
16. Cheng, L., Stys, D., and Allen, J. F. (1995) *Physiol. Plant.* **93,** 173–178
17. Burke, J. J., Ditto, C. L., and Arntzen, C. J. (1978) *Arch. Biochem. Biophys.* **187,** 252–263
18. Kühlbrandt, W., Thaler, T. H., and Wehrli, E. (1983) *J. Cell Biol.* **96,** 1414–1424
19. Yang, J. T., Wu, C. S., and Martinez, H. M. (1986) *Methods Enzymol.* **130,** 208–269
20. Hobe, S., Prytulla, S., Kühlbrandt, W., and Paulsen, H. (1994) *EMBO J.* **13,** 3423–3429
21. Bax, A., and Davis, D. G. (1985) *J. Magn. Reson.* **65,** 355–360
22. Bax, A., Griffey, R. H., and Hawkins, B. L. (1983) *J. Magn. Reson.* **55,** 301–307
23. Kumar, A., Hosur, R. V., and Chandrasekhar, K. (1984) *J. Magn. Reson.* **60,** 143–148
24. Wüthrich, K. (1986) *NMR of Proteins and Nucleic Acids*, Wiley Interscience, New York
25. Surewicz, W. K., Mantsch, H. H., and Chapman, D. (1993) *Biochemistry* **32,** 389–394
26. Krimm, S., and Bandekar, J. (1986) *Adv. Protein Chem.* **38,** 181–364
27. Wilder, C. L., Friedrich, A. D., Potts, R. O., Daumy, G. O., and Francoeur, M. L. (1992) *Biochemistry* **31,** 27–31
28. Byler, D. M., and Susi, H. (1986) *Biopolymers* **25,** 469–487
29. Jackson, M., and Mantsch, H. H. (1995) *Crit. Rev. Biochem. Mol. Biol.* **30,** 95–120
30. Torii, H., and Tasumi, M. (1992) *J. Chem. Phys.* **96,** 3379–3387
31. Venyaminov, S. Y., and Kalnin, N. N. (1990) *Biopolymers* **30,** 1243–1257
32. Venyaminov, S. Y., and Kalnin, N. N. (1990) *Biopolymers* **30,** 1259–1271
33. Kalnin, N. N., Baikalov, I. A., and Venyaminov, S. Y. (1990) *Biopolymers* **30,** 1273–1280
34. Giuffra, E., Cugini, D., Croce, R., and Bassi, R. (1996) *Eur. J. Biochem.* **238,** 112–120
35. Otvos, L., Jr., Thurin, J., Kollat, E., Urge, L., Mantsch, H. H., and Hollosi, M. (1991) *Int. J. Pept. Protein Res.* **38,** 476–482
36. Fabian, H., Otvos, L., Jr., Szendrei, G. I., Lang, E., and Mantsch, H. H. (1994) *J. Biomol. Struct. & Dyn.* **12,** 573–579
37. Augusteyn, R. C., Koretz, J. F., and Schurtenberger, P. (1989) *Biochim. Biophys. Acta* **999,** 293–299
38. Ramwani, J. J., Epand, R. M., and Moscarello, M. A. (1989) *Biochemistry* **28,** 6538–6543
39. Mortishire-Smith, R. J., Pitzenberger, S. M., Burke, C. J., Middaugh, C. R., Garsky, V. M., and Johnson, R. G. (1995) *Biochemistry* **34,** 7603–7613
40. Buelt, M. K., Xu, Z., Banaszak, L. J., and Bernlohr, D. A. (1992) *Biochemistry* **31,** 3493–3499
41. Rajagopal, P., Waygood, E. B., and Klevit, R. E. (1994) *Biochemistry* **33,** 15271–15282
42. Otvos, L., Jr., Hollosi, M., Perczel, A., Dietzschold, B., and Fasman, G. D. (1988) *J. Protein Chem.* **7,** 365–376
43. Croce, R., Breton, J., and Bassi, R. (1996) *Biochemistry* **35,** 11142–11148
44. Nussberger, S., Dörr, K., Wang, D. N., and Kühlbrandt, W. (1993) *J. Mol. Biol.* **234,** 347–356
45. Lindblom, G., and Rilfors, L. (1989) *Biochim. Biophys. Acta* **988,** 221–256
46. Paulsen, H., and Kuttkat, A. (1993) *Photochem. Photobiol.* **57,** 139–142
47. Barford, D., Hu, S.-H., and Johnson, L. N. (1991) *J. Mol. Biol.* **218,** 233–260
48. Pribic, R., van Stokkum, I. H., Chapman, D., Haris, P. I., and Bloemendal, M. (1993) *Anal. Biochem.* **214,** 366–378
49. Williams, K. A., and Deber, C. M. (1991) *Biochemistry* **30,** 8919–8923
50. Ludlam, C. F., Sonar, S., Lee, C. P., Coleman, M., Herzfeld, J., RajBhandary, U. L., and Rothschild, K. J. (1995) *Biochemistry* **34,** 2–6
51. Vanhoff, G., Goossens, F., De Meester, I., Hendriks, D., and Scharpé, S. (1995) *FASEB J.* **9,** 736–744
52. Barber, J. (1982) *Annu. Rev. Plant. Physiol.* **33,** 261–295
53. Wollman, F.-A., and Diner, B. (1980) *Arch. Biochem. Biophys.* **201,** 646–658
54. Kohorn, B. D., and Yakir, D. (1990) *J. Biol. Chem.* **265,** 2118–2123
55. Allen, J. F. (1992) *Trends Biochem. Sci.* **17,** 12–17
56. Stys, D. (1995) *Physiol. Plant.* **95,** 651–657
57. Wu, W.-G., and Huang, C.-H. (1981) *Lipids* **6,** 820–822
58. Matthews, B. W., Fenna, R. E., Bolognesi, M. C., Schmid, M. F., and Olson, J. M. (1979) *J. Mol. Biol.* **131,** 259–285
59. Dürring, M., Schmidt, G. B., and Huber, R. (1991) *J. Mol. Biol.* **217,** 577–592
60. McDermott, G., Prince, S. M., Freer, A. A., Hawthornwaite-Lawless, A. M., Papiz, M. Z., Cogdell, R. J., and Isaacs, N. W. (1995) *Nature* **374,** 517–521
61. Allen, J. P., Feher, G., Yeates, T. O., Komiya, H., and Rees, D. C. (1987) *Proc. Natl. Acad. Sci. U. S. A.* **84,** 6162–6166
62. Allen, J. P., Feher, G., Yeates, T. O., Komiya, H., and Rees, D. C. (1987) *Proc. Natl. Acad. Sci. U. S. A.* **84,** 5730–5734
63. Kraub, N., Schubert, W.-D., Klukas, O., Fromme, P., Witt, H. T., and Saenger, W. (1996) *Nat. Struct. Biol.* **3,** 965–973
64. Schreuder, H. A., Knight, S., Curmi, P. M., Andersson, I., Cascio, D., Sweet, R. M., Bränden, C. I., and Eisenberg, D. (1993) *Protein Sci.* **2,** 1136–1146
65. Schneider, G., Knight, S., Andersson, I., Bränden, C. I., Lindqvist, Y., and Lundqvist, T. (1990) *EMBO J.* **9,** 2045–2050
66. Kauppinen, J. K., Moffatt, D. J., Mantsch, H. H., and Cameron, D. G. (1981) *Appl. Spectrosc.* **35,** 271–276